

Microwave Engineering & Applications

Om Gandhi

Pergamon Press © 1981

CHAPTER IV

MICROWAVE WAVEGUIDES

4.1 Introduction

The general relationships for TE and TM waves in single conductor waveguides were derived in Section 2.3. It was shown that the field components are derivable from H_z and E_z , respectively, which in turn satisfy the wave equation in the filler medium subject to the metallic boundary conditions. It was also shown that the transverse fields \vec{E}_t , \vec{H}_t are at right angles to one another at all points in the transverse plane and are oriented such that \vec{E}_t , \vec{H}_t , and \hat{z} form a right-handed coordinate system. The important relationships for TE and TM modes of a waveguide are summarized in Section 2.6. Waveguides of rectangular and circular cross section are the ones that are most commonly used, and these are consequently discussed at length in this chapter.

Also discussed in Section 4.13 is a computer program for transmission line/waveguide problems.

4.2 TE and TM Modes in a Rectangular Waveguide

The schematic of a rectangular waveguide which is a hollow metallic pipe of rectangular cross section is shown in Fig. 4.1. The longer and shorter inside

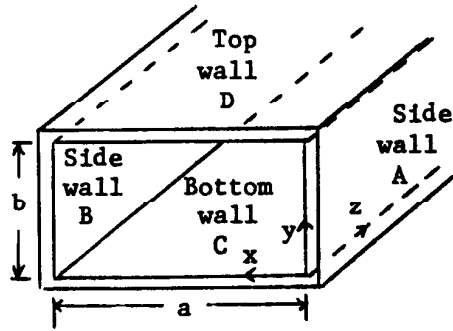


Fig. 4.1. Schematic diagram of a rectangular waveguide.

dimensions of the waveguide cross section are represented by a and b , respectively. Because of a very small skin depth ($\sim 10^{-4}$ cm), the outside dimensions are unimportant to the propagation of fields in such a system. Plastic waveguides that are coated on the inside with highly conducting materials are perfectly capable of propagating microwaves as good as metallic waveguides.

Being a single conductor system, a rectangular waveguide is not capable of supporting TEM waves which require waveguides of two or more conductors. Propagation down to zero frequencies is consequently not possible in a rectangular waveguide (see Section 2.6). In this section we will show that energy propagation in a rectangular waveguide is possible only for frequencies in excess of $c_e/2a$.

In the following we use the general relationships of Section 2.6 to solve for fields in a rectangular waveguide.

Transverse Electric or TE Waves

$$E_z = 0 \quad (4.1)$$

Solve for H_z from the wave equation

$$\nabla^2 H_z + k_\epsilon^2 H_z = 0 \quad (4.3)$$

$$\frac{\partial^2 H_z}{\partial x^2} + \frac{\partial^2 H_z}{\partial y^2} + \frac{\partial^2 H_z}{\partial z^2} + k_\epsilon^2 H_z = 0 \quad (4.5)$$

Transverse Magnetic or TM Waves

$$H_z = 0 \quad (4.2)$$

Solve for E_z from the wave equation

$$\nabla^2 E_z + k_\epsilon^2 E_z = 0 \quad (4.4)$$

$$\frac{\partial^2 E_z}{\partial x^2} + \frac{\partial^2 E_z}{\partial y^2} + \frac{\partial^2 E_z}{\partial z^2} + k_\epsilon^2 E_z = 0 \quad (4.6)$$

We are looking for propagating solutions; i.e., the z -variation is of the type $e^{-j\beta z}$. Substituting this, then, in the above equations,

$$\frac{\partial^2 H_z}{\partial x^2} + \frac{\partial^2 H_z}{\partial y^2} + (k_\epsilon^2 - \beta^2) H_z = 0 \quad (4.7)$$

$$\frac{\partial^2 E_z}{\partial x^2} + \frac{\partial^2 E_z}{\partial y^2} + (k_\epsilon^2 - \beta^2) E_z = 0 \quad (4.8)$$

These are second-order partial differential equations which may be solved by separation of variables:

$$H_z = X(x) Y(y) e^{j(\omega t - \beta z)} \quad (4.9)$$

where X and Y are functions of variables x and y , respectively.

$$E_z = X'(x) Y'(y) e^{j(\omega t - \beta z)} \quad (4.10)$$

X' and Y' are some different functions of variables x and y , respectively.

Upon substituting in Eqs. 4.7 and 4.8, respectively, to obtain the nature of the functions X , Y , X' , and Y' , we get:

$$\frac{1}{Y} \frac{d^2 Y}{dy^2} + \gamma^2 = -\frac{1}{X} \frac{d^2 X}{dx^2} \quad (4.11)$$

$$\frac{1}{Y'} \frac{d^2 Y'}{dy^2} + \gamma^2 = -\frac{1}{X'} \frac{d^2 X'}{dx^2} \quad (4.12)$$

$$\text{where } \gamma^2 = k_c^2 - \beta^2 = \left(\frac{m\pi}{a}\right)^2 + \left(\frac{n\pi}{b}\right)^2$$

Since the right sides of Eqs. 4.11 and 4.12 are functions of variable x alone, and the left sides are functions of variable y alone, and yet the equations are to be satisfied for all x and y , that would be possible only if each side equals a constant which may be called k_x^2 for Eq. 4.11 and $k_x'^2$ for Eq. 4.12, in which case:

$$H_z = (A \cos k_x x + B \sin k_x x) \cdot (C \cos k_y y + D \sin k_y y) e^{j(\omega t - \beta z)} \quad (4.13)$$

where

$$k_y^2 = \gamma^2 - k_x^2 \quad (4.15)$$

$$E_z = (A' \cos k_x' x + B' \sin k_x' x) \cdot (C' \cos k_y' y + D' \sin k_y' y) e^{j(\omega t - \beta z)} \quad (4.14)$$

and

$$k_y'^2 = \gamma^2 - k_x'^2 \quad (4.16)$$

The boundary conditions to be satisfied at the metallic walls are:

$$\frac{\partial H_z}{\partial n} = \frac{\partial H_z}{\partial x} = 0 \text{ for all } y \quad (4.17)$$

at $x = 0$ and at $x = a$ corresponding to right- and left-side walls A and B (Fig. 4.1), respectively:

$$\frac{\partial H_z}{\partial n} = \frac{\partial H_z}{\partial y} = 0 \text{ for all } x \quad (4.19)$$

at $y = 0$ and at $y = b$ corresponding to the bottom and top walls C and D (Fig. 4.1), respectively.

$$E_z = 0 \text{ for all } y \quad (4.18)$$

at $x = 0$ and $x = a$ for right- and left-side walls A and B, respectively.

$$E_z = 0 \text{ for all } x \quad (4.20)$$

at $y = 0$ and $y = b$ for bottom and top walls C and D, respectively.

TE modes

TM modes

Upon substituting the above boundary conditions in equations, we obtain:

$$H_z = H_{mn} \cos \frac{m\pi x}{a} \cos \frac{n\pi y}{b} e^{j(\omega t - \beta z)} \quad (4.21)$$

$$E_z = E_{mn} \sin \frac{m\pi x}{a} \sin \frac{n\pi y}{b} e^{j(\omega t - \beta z)} \quad (4.22)$$

where, of course, all integer values of m and n are allowable. While m or n (but not both) may be zero in Eq. 4.21, neither m nor n may be zero in Eq. 4.22 because that would make $E_z = 0$ and, from Eqs. 2.65 and 2.66 for TM waves, \vec{E}_t and \vec{H}_t would both be zero, which is a trivial solution (completely zero electric and magnetic fields).

For given values of m and n from Eqs. 4.15 and 4.16, we obtain:

$$k_\epsilon^2 - \beta^2 = k_x^2 + k_y^2 = \frac{m^2 \pi^2}{a^2} + \frac{n^2 \pi^2}{b^2} \quad (4.23)$$

$\epsilon = \frac{1}{\mu \epsilon} = 3E8$ for air

$$k_\epsilon^2 - \beta^2 = k_x'^2 + k_y'^2 = \frac{m^2 \pi^2}{a^2} + \frac{n^2 \pi^2}{b^2} \quad (4.24)$$

or

$$\frac{\omega}{c_\epsilon} \sqrt{\beta^2 - f_{mn}^2} = \beta = \sqrt{\frac{\omega^2}{c_\epsilon^2} - \left(\frac{m^2 \pi^2}{a^2} + \frac{n^2 \pi^2}{b^2} \right)} \quad (4.25)$$

or

$$\beta = \sqrt{\frac{\omega^2}{c_\epsilon^2} - \left(\frac{m^2 \pi^2}{a^2} + \frac{n^2 \pi^2}{b^2} \right)} \quad (4.26)$$

The propagation constant β is real only for frequencies larger than or equal to:

$$f_c \geq \frac{c_\epsilon}{2} \sqrt{\left(\frac{m^2}{a^2} + \frac{n^2}{b^2} \right)} \quad (4.27)$$

$$f \geq \frac{c_\epsilon}{2} \sqrt{\left(\frac{m^2}{a^2} + \frac{n^2}{b^2} \right)} \quad (4.28)$$

The lowest frequency TE_{mn} mode propagation (since $a > b$) corresponds to the TE_{10} mode which is possible for frequencies higher than or equal to:

$$f_{10} = \frac{c_\epsilon}{2a} \quad (4.29)$$

The lowest frequency TM_{mn} mode propagation corresponds to TM_{11} mode (since $m \neq 0$ and $n \neq 0$, as discussed above) and the cutoff frequency for this mode is:

$$f_{11} = \frac{c_\epsilon}{a} \sqrt{\left(\frac{1}{a^2} + \frac{1}{b^2} \right)} \quad (4.30)$$

The cutoff frequency of a given mode is that frequency below which β is imaginary; i.e., the wave is an evanescent wave. The wave amplitudes decay rather rapidly with distance. The cutoff frequencies of TE_{mn} and TM_{mn} modes are identical, these being

cutoff frequency

For Rectangular Waveguide only

$$f_{mn} = \frac{c_\epsilon}{2} \sqrt{\left(\frac{m^2}{a^2} + \frac{n^2}{b^2} \right)} \quad (4.31)$$

↑ meters

Hz

The subscripts m and n in the nomenclature for TE and TM modes represent the

$$a^2 > b^2$$

number of half (sinusoidal) cycles of variation of fields along x and y dimensions, respectively. It should be remembered that even though the wave propagation constants are identical (from Eqs. 4.25 and 4.26) for TE and TM modes for given values of m and n, i.e., the two modes propagate at the same velocity, the field patterns, as will be shown in the following, are radically different, and hence there is no confusion in the kind of fields that need to be excited if TE_{mn} or TM_{mn} mode excitation is desired.

In the following $e^{j(\omega t - \beta z)}$ would be implied in all fields and hence not written repetitiously.

From Eq. 4.21:

$$\boxed{H_z} = H_{mn} \cos \frac{m\pi x}{a} \cos \frac{n\pi y}{b} e^{j(\omega t - \beta z)} \quad (4.32)$$

From Eq. 4.22:

$$\boxed{E_z} = E_{mn} \sin \frac{m\pi x}{a} \sin \frac{n\pi y}{b} e^{j(\omega t - \beta z)} \quad (4.33)$$

Having solved for H_z and E_z , it should now be possible to write the transverse components of fields from the general equations of Section 2.6.

From Eqs. 2.61 and 2.62:

$$\begin{aligned} \vec{H}_t &= \frac{-j\beta}{\gamma^2} \vec{\nabla}_t H_z \\ &= \frac{-j\beta}{\gamma^2} \left(\frac{\partial H_z}{\partial x} \hat{x} + \frac{\partial H_z}{\partial y} \hat{y} \right) \end{aligned} \quad (4.34)$$

$$\vec{E}_t = \frac{\omega\mu}{\beta} \vec{H}_t \times \hat{z} = Z_{TE} \vec{H}_t \times \hat{z} \quad (4.36)$$

where

$$Z_{TE} = \frac{377/\sqrt{\epsilon_r}}{1 - (f/f_c)^2} \quad \text{freq. depend - variation independent}$$

$$\boxed{\gamma^2} = \frac{m^2 \pi^2}{a^2} + \frac{n^2 \pi^2}{b^2} \quad (4.38)$$

$$\boxed{H_x} = \frac{j\beta}{\gamma^2} \frac{m\pi}{a} H_{mn} \sin \frac{m\pi x}{a} \cos \frac{n\pi y}{b} e^{j(\omega t - \beta z)} \quad (4.40)$$

$$\boxed{H_y} = \frac{j\beta}{\gamma^2} \frac{n\pi}{b} H_{mn} \cos \frac{m\pi x}{a} \sin \frac{n\pi y}{b} e^{j(\omega t - \beta z)} \quad (4.42)$$

$$\boxed{E_x} = Z_{TE} H_y \quad (4.44)$$

$$\boxed{E_y} = -Z_{TE} H_x \quad (4.46)$$

From Eqs. 2.65 and 2.66:

$$\begin{aligned} \vec{E}_t &= \frac{-j\beta}{\gamma^2} \vec{\nabla}_t E_z \\ &= \frac{-j\beta}{\gamma^2} \left(\frac{\partial E_z}{\partial x} \hat{x} + \frac{\partial E_z}{\partial y} \hat{y} \right) \end{aligned} \quad (4.35)$$

$$\vec{H}_t = \frac{\omega\epsilon}{\beta} \hat{z} \times \vec{E}_t = \frac{\hat{z} \times \vec{E}_t}{Z_{TM}} \quad (4.37)$$

$$\boxed{\gamma^2} = \frac{m^2 \pi^2}{a^2} + \frac{n^2 \pi^2}{b^2} \quad (4.39)$$

$$\boxed{E_x} = \frac{-j\beta}{\gamma^2} \frac{m\pi}{a} E_{mn} \cos \frac{m\pi x}{a} \sin \frac{n\pi y}{b} e^{j(\omega t - \beta z)} \quad (4.41)$$

$$\boxed{E_y} = \frac{-j\beta}{\gamma^2} \frac{n\pi}{b} E_{mn} \sin \frac{m\pi x}{a} \cos \frac{n\pi y}{b} e^{j(\omega t - \beta z)} \quad (4.43)$$

$$\boxed{H_x} = -\frac{E_y}{Z_{TM}} \quad (4.45)$$

$$\boxed{H_y} = \frac{E_x}{Z_{TM}} \quad (4.47)$$

The various electric and magnetic field components associated with the TE_{mn} and TM_{mn} modes of a rectangular waveguide are now known and may be seen to be completely different for the two modes. The electric and magnetic field configurations of a few TE and TM modes of a rectangular waveguide are shown in Fig. 4.2. In the diagrams the electric fields are sketched in bold lines while the magnetic field lines are shown in broken lines. The reader is advised to look at the field expressions for a selected mode and see for himself the validity of the plots in Fig. 4.2.

4.3 Bouncing Wave Picture of Wave Propagation in Waveguides

By looking at the nature of the wave fields in Eqs. 4.32 to 4.47, we can see that these may be visualized in terms of a plane wave bouncing back and forth between the various waveguide walls. To illustrate the point, let us consider the case of TE_{m0} fields.

For the TE_{m0} mode, the fields are:

$$E_y = -j\omega\mu \frac{a}{m\pi} H_{m0} \sin \frac{m\pi x}{a} e^{j(\omega t - \beta z)} \quad (4.48)$$

$$H_x = \frac{-E_y}{(\omega\mu/\beta)} = j\beta \frac{a}{m\pi} H_{m0} \sin \frac{m\pi x}{a} e^{j(\omega t - \beta z)} \quad (4.49)$$

$$H_z = H_{m0} \cos \frac{m\pi x}{a} e^{j(\omega t - \beta z)} \quad (4.50)$$

$$H_y = E_x = E_z \equiv 0 \quad (4.51)$$

$$\beta = \sqrt{\frac{\omega^2}{c^2} - \frac{m^2 \pi^2}{a^2}} = \frac{2\pi f}{c} \sqrt{1 - \left(\frac{f_{m0}}{f}\right)^2} \quad (4.52)$$

where $f_{m0} = mc_\epsilon/2a$ is the cutoff frequency of the TE_{m0} mode (see Eq. 4.27).

Equation 4.48 can be written in terms of equal amplitude incident and reflected plane waves (sketched in Fig. 4.3):

$$\begin{aligned} \vec{E} &= \vec{E}_{inc} + \vec{E}_{refl} \\ &= E_1 \hat{y} \left[e^{j(\omega t - k_\epsilon \cos \theta x - k_\epsilon \sin \theta z)} - e^{j(\omega t + k_\epsilon \cos \theta x - k_\epsilon \sin \theta z)} \right] \\ &= 2jE_1 \hat{y} \sin(k_\epsilon \cos \theta x) e^{j(\omega t - k_\epsilon \sin \theta z)} \end{aligned} \quad (4.53)$$

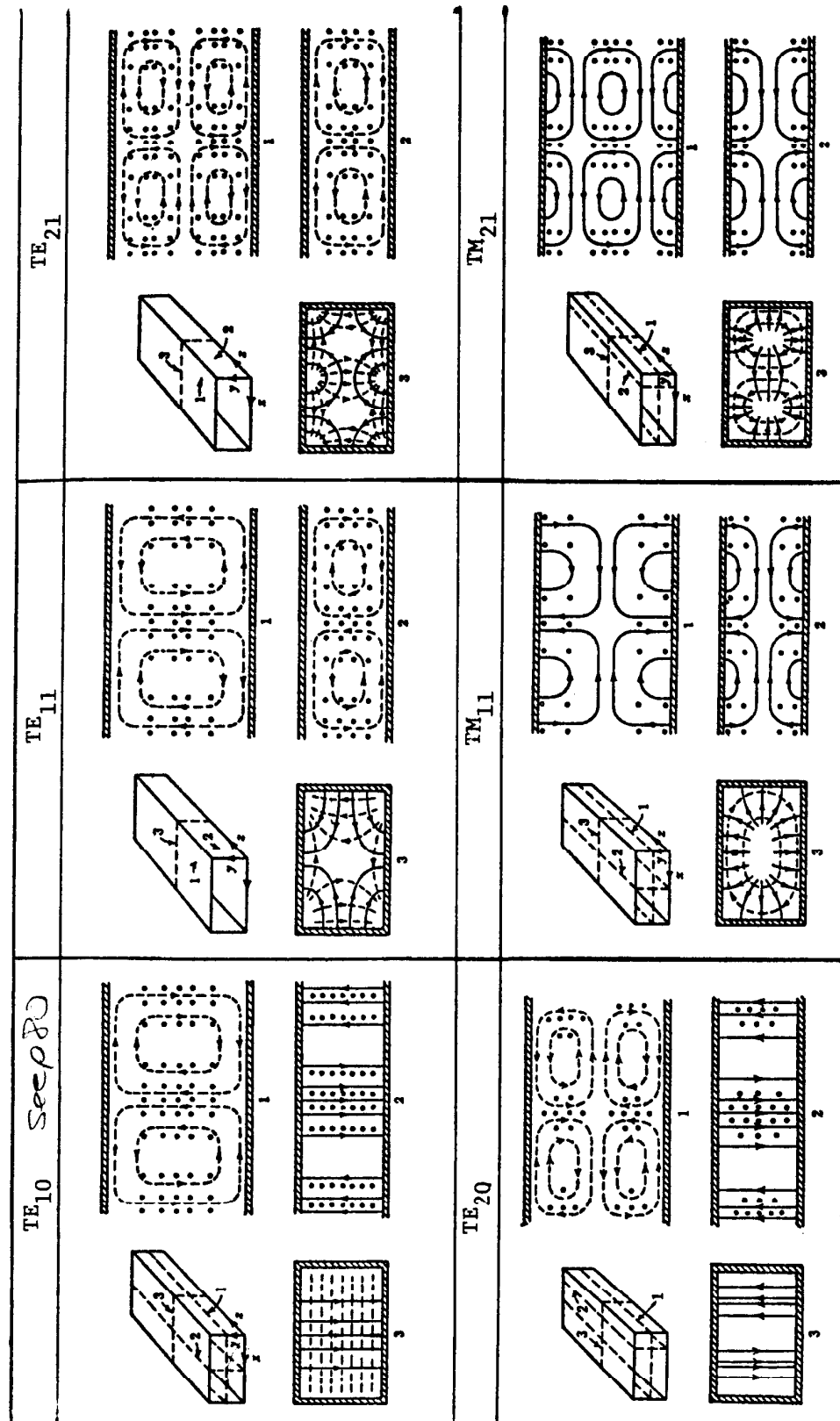


Fig. 4.2. Field patterns of some modes of a rectangular waveguide. [Source: S. Ramo, J. R. Whinnery, and T. Van Duzer, Ref. 1.]

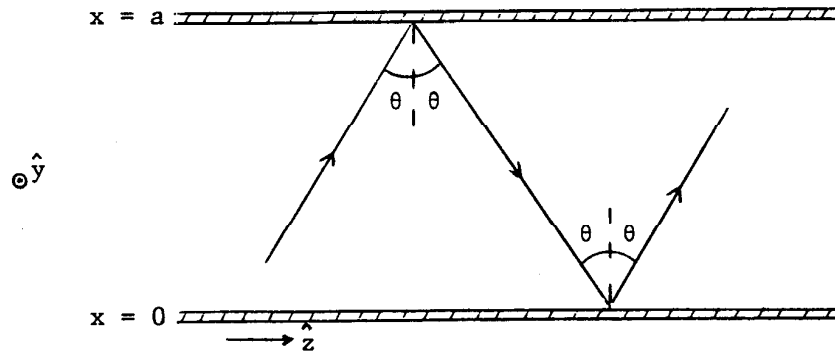


Fig. 4.3. Bouncing wave picture of wave propagation in rectangular waveguide, top view.

Expression 4.53 for plane waves bouncing back and forth between the two side walls of the rectangular waveguide is identical to the electric field (Eq. 4.48) of the TE_{m0} wave. Also, since the tangential electric field at the side walls $x = 0$ and $x = a$ is zero,

$$\cos \theta = \frac{f_c}{f} \quad \sin \theta = \sqrt{1 - \cos^2 \theta} \quad \lambda_g = \frac{\lambda_e}{\sin \theta} \quad k_e \cos \theta a = m\pi \quad (4.54)$$

and $k_e \sin \theta$ is equal to β , the wave propagation constant, in which case,

$$\beta^2 = k_e^2 (1 - \cos^2 \theta) = k_e^2 - m^2 \pi^2 / a^2 = (\omega^2 / c_e^2) (1 - f_{m0}^2 / f^2) \quad (4.55)$$

Equation 4.54 defines θ the angle of incidence (and reflection) of the plane wave/s. θ is zero for $f = f_{m0}$, the cutoff frequency, which means that at cutoff the wave bounces back and forth without any forward motion. θ increases as frequencies larger than the cutoff frequency are propagated down the waveguide.

Similar visualization is also possible for TE_{mn} and TM_{mn} modes with a plane wave making a finite angle relative to the xz plane (depicted in Fig. 4.3).

4.4 Wave Velocities

Phase Velocity

Phase velocity v_p of a wave is defined as the velocity of a point of constant phase. For waves in the waveguide, the points of constant phase correspond to

$$\omega t - \beta z = \text{constant } K \quad (4.56)$$

At time $t + dt$, the same constant phase point has moved to $z + dz$ such that

$$\omega(t + dt) - \beta(z + dz) = K \quad (4.57)$$

in which case the velocity of movement of the constant phase point

$$v_p \equiv \frac{dz}{dt} = \frac{\omega}{\beta} \quad (4.58)$$

For TE_{mn} or TM_{mn} modes, therefore,

$$v_p = c_\epsilon / \sqrt{1 - \frac{f_{mn}^2}{f^2}} \quad \text{Phase Velocity} \quad (4.59)$$

which is always larger than the velocity of light c_ϵ and approaches c_ϵ as frequencies much larger than the cutoff frequency f_{mn} are propagated. This is represented in Fig. 4.4. It should be remembered at this stage that the phase

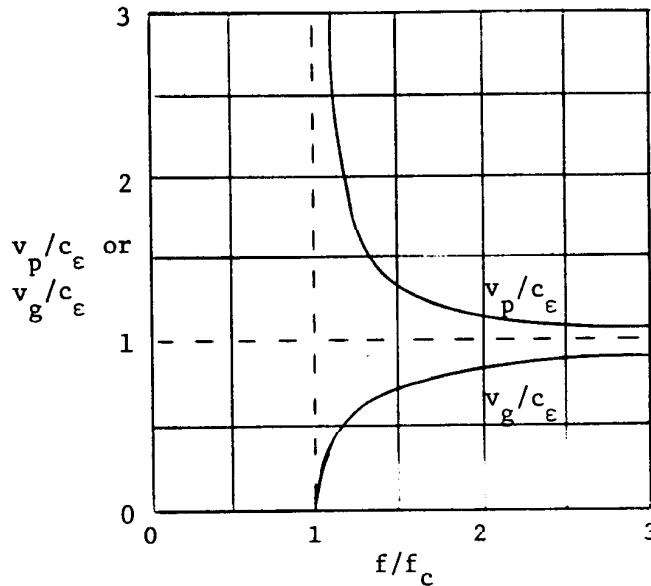


Fig. 4.4. Phase and group velocity characteristics of guided waves.

velocity is not the energy propagation velocity which must always be less than or equal to c_ϵ . The phase velocity is comparable to the velocity at which, say, the peak of a ripple (constant phase point) moves along the bank of a water pond. The peak of a ripple would easily be moving at a velocity much larger than the velocity of water movement in the pond because different elements of water are experiencing the ripple peak at different times. In fact, the water in the pond may barely be moving in the horizontal direction and yet the ripple could be moving at a very fast speed.

Group Velocity

The *group velocity* v_g of a wave is the velocity at which the energy (signal information) consisting of a finite (rather than zero) frequency region of the spectrum propagates.

A general input signal $f_1(t)$ can be written in terms of various frequency components by the use of the Fourier transforms

$$f_1(t) = \frac{1}{2\pi} \int_{-\infty}^{\infty} F_1(\omega) e^{j\omega t} d\omega \quad (4.60)$$

where

$$F_1(\omega) = \int_{-\infty}^{\infty} f_1(t) e^{-j\omega t} dt \quad (4.61)$$

The above equations are counterparts to discrete Fourier series where a given signal, if composed of discrete frequency components, can be expressed as $\sum F_1(\omega) e^{j\omega t}$.

In propagating down a waveguide, the various frequency components of the signal undergo different amounts of phase shift $e^{-j\beta(\omega)z}$ and the spectral distribution $F_o(\omega)$ of the signal at output, neglecting attenuation of the various frequency components, is given by:

$$F_o(\omega) = F_1(\omega) e^{-j\beta(\omega)z} \quad (4.62)$$

If the bandwidth of the signal is rather narrow and is centered at ω_1 , we can expand $\beta(\omega)$ around ω_1

$$\beta(\omega) \approx \beta_o(\omega_1) + \left. \frac{d\beta}{d\omega} \right|_{\omega_1} (\omega - \omega_1) \quad (4.63)$$

Substituting this in Eq. 4.62, the time variation of the output signal $f_o(t)$ is written from the inverse-Fourier-transform of Eq. 4.62:

$$\begin{aligned} f_o(t) &= \frac{e^{j(\omega_1 t - \beta_o z)}}{2\pi} \int_{-\infty}^{\infty} F_1(\omega) e^{j(\omega - \omega_1) \left(t - \left. \frac{d\beta}{d\omega} \right|_{\omega_1} z \right)} d(\omega - \omega_1) \\ &= f_1(t - t_a) e^{j(\omega_1 t - \beta_o z)} \end{aligned} \quad (4.64)$$

where $t_a = \left. \frac{d\beta}{d\omega} \right|_{\omega_1} z$.

The output therefore is the delayed version of the input waveshape which is delayed in phase, too, by $e^{j\beta_o z}$.

The velocity of signal propagation v_g can now be derived from the delay time in

propagating a distance z and v_g is given by:

$$v_g = \left. \frac{d\omega}{d\beta} \right|_{\omega_i} \quad (4.65)$$

For TE_{mn} or TM_{mn} modes, therefore,

group
velocity

$$v_g = c_\epsilon \sqrt{1 - f_{mn}^2/f^2} \quad (4.66)$$

In waveguides the group velocity at a frequency f is always less than or equal to c_ϵ . The variation of v_g with frequency is also plotted in Fig. 4.4. It can be seen that for any frequency the product $v_p v_g = c_\epsilon^2$.

4.5 Some Important Relationships for (Single Conductor) Waveguides

valid for all
waveguide shapes

$$\beta = 2\pi/\lambda_g = \frac{\sqrt{\omega^2 - \omega_c^2}}{c_\epsilon} \quad (4.67)$$

where λ_g is the guide wavelength or the separation between identical phase points at a given instant of time.

guide
wavelength

$$\lambda_g = \frac{c_\epsilon}{f} \frac{1}{\sqrt{1 - f_c^2/f^2}} = \frac{\lambda_\epsilon}{\sqrt{1 - f_c^2/f^2}} = \frac{2\pi}{\beta} > \lambda_\epsilon \quad (4.68)$$

$c_\epsilon/f = \frac{\lambda_0}{\sqrt{\epsilon_r}}$

where $\lambda_\epsilon = c_\epsilon/f$ is the wavelength at the signal frequency for electromagnetic waves in an infinite medium having the permittivity of the filler material of the waveguide. $\lambda_\epsilon = \lambda_0$ for air-filled waveguides.

f_c is the cutoff frequency for the mode under consideration. For rectangular waveguides,

* For Only
Rectangular
Waveguides

$$f_c|_{TE_{mn}} = f_c|_{TM_{mn}} = c_\epsilon \sqrt{\left(\frac{m}{2a}\right)^2 + \left(\frac{n}{2b}\right)^2} \quad (4.69)$$

It is a special feature of rectangular waveguides that the cutoff frequencies for TE_{mn} and TM_{mn} modes (not their fields) are identical. This is not so in any other geometry, including that for circular waveguides.

$$Z_{TE} = \frac{\omega\mu}{\beta} = \frac{377/\sqrt{\epsilon_r}}{\sqrt{1 - f_c^2/f^2}} = \frac{|E_y|}{|H_x|} = 377 \frac{\lambda_g}{\lambda_\epsilon} \quad (4.70)$$

$$Z_{TM} = \frac{\beta}{\omega\epsilon} = \frac{377}{\sqrt{\epsilon_r}} \sqrt{1 - \frac{f_c^2}{f^2}} \quad (4.71)$$

$$v_p = \frac{\omega}{\beta} = \frac{c_\epsilon}{\sqrt{1 - f_c^2/f^2}} \quad (4.72)$$

$$v_g = \frac{d\omega}{d\beta} = \frac{c_\epsilon^2}{v_p} = c_\epsilon \sqrt{1 - \frac{f_c^2}{f^2}} \quad (4.73)$$

4.6 The Lowest Frequency Mode — TE_{10} Mode — of a Rectangular Waveguide

Of the TE_{mn} or TM_{mn} modes of a rectangular waveguide, the TE_{10} mode has the lowest cutoff frequency which is given by $c_\epsilon/2a$. The next higher order mode is TE_{20} (and TE_{01} mode for waveguides where $b = a/2$), having the cutoff frequency twice as much; i.e., c_ϵ/a . In several waveguides, the smaller dimension b is slightly smaller than $a/2$, which removes the coalescence of the cutoff frequencies of the TE_{20} and TE_{01} modes and places the TE_{01} mode at a cutoff frequency $c_\epsilon/2b$ slightly larger than c_ϵ/a of the TE_{20} mode. Since the propagation of various modes is possible for all frequencies higher than the cutoff frequency of that mode, one and only one mode of propagation is possible only for $c_\epsilon/2a < f < c_\epsilon/a$ for the TE_{10} mode. In this frequency region, other modes of the rectangular waveguide, if excited, say, because of a discontinuity or deformation (including burrs, etc.), will not propagate very far because of imaginary β and single mode of propagation would therefore persist in the waveguide. Multimode propagation at higher frequencies has the disadvantage that the various modes propagate at differing phase velocities, causing interference. The TE_{10} mode of the rectangular waveguide is used most often, therefore, to ensure single mode propagation.

The dimension a of the waveguide is therefore picked so that the signal frequency is at least 15-20 percent higher than the cutoff frequency $c_\epsilon/2a$ and no more than 90-95 percent of the cutoff frequency of the TE_{20} mode. Putting it another way, the recommended operating range of a rectangular waveguide is:

To choose waveguide dimensions)

$$(1.15-1.2) \frac{c_\epsilon}{2a} \leq f \leq (0.9-0.95) \frac{c_\epsilon}{a} \quad (4.74)$$

$f_{c|TE_{10}}$ $f_{c|TE_{20}}$

The salient features of some commercially available waveguides are given in Table 4.1.

The waveguide attenuation for some rectangular waveguides is shown in Fig. 4.5.

The fields associated with the TE_{10} mode are given in Eqs. 4.48 to 4.51 (for $m = 1$). The fields are sketched in Fig. 4.6. A convenient way to excite this mode

Choose a so $f_c \leq .8f$

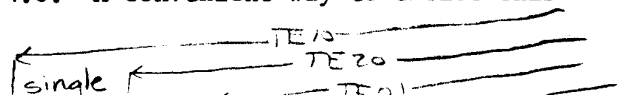


TABLE 4.1. Salient features of some commercially available rectangular waveguides.

EIA Designation WR()	Inside Dimensions (Inches)		TE_{10} Cutoff Frequency $c/2a$ GHz	Recommended Frequency Range for TE_{10} Mode GHz $1.25f_{10} \leq f \leq .95f_{20}$	Theoretical CW Power Rating for Lowest to Highest Frequency MW
	a, b	Tolerance + or -			
2300	23.000-11.500	.020	0.256	0.32-0.49	153.0-212.0
2100	21.000-10.500	.020	0.281	0.35-0.53	120.0-173.0
1800	18.000-9.000	.020	0.328	0.41-0.625	93.4-131.9
1500	15.000-7.500	.015	0.393	0.49-0.75	67.6-93.3
1150	11.500-5.750	.015	0.513	0.64-0.96	35.0-53.8
975	9.750-4.875	.010	0.605	0.75-1.12	27.0-38.5
770	7.700-3.850	.005	0.766	0.96-1.45	17.2-24.1
650	6.500-3.250	.005	0.908	1.12-1.70	11.9-17.2
510	5.100-2.550	.005	1.157	1.45-2.20	7.5-10.7
430	4.300-2.150	.005	1.372	1.70-2.60	5.2-7.5
340	3.400-1.700	.005	1.736	2.20-3.30	3.1-4.5
284	2.840-1.340	.005	2.078	2.60-3.95	2.2-3.2
229	2.290-1.145	.005	2.577	3.30-4.90	1.6-2.2
187	1.872-0.872	.005	3.152	3.95-5.85	1.4-2.0
159	1.590-0.795	.004	3.711	4.90-7.05	0.79-1.0
137	1.372-0.622	.004	4.301	5.85-8.20	0.56-0.71
112	1.122-0.497	.004	5.259	7.05-10.00	0.35-0.46
90	0.900-0.400	.003	6.557	8.20-12.40	0.20-0.29
75	0.750-0.375	.003	7.868	10.00-15.00	0.17-0.23
62	0.622-0.311	.0025	9.486	12.40-18.00	0.12-0.16
51	0.510-0.255	.0025	11.574	15.00-22.00	0.080-0.107
42	0.420-0.170	.002	14.047	18.00-26.50	0.043-0.058
34	0.340-0.170	.002	17.328	22.00-33.00	0.034-0.048
28	0.280-0.140	.0015	21.081	26.50-40.00	0.022-0.031
22	0.224-0.112	.001	26.342	33.00-50.00	0.014-0.020
19	0.188-0.094	.001	31.357	40.00-60.00	0.011-0.015
15	0.148-0.074	.001	39.863	50.00-75.00	0.0063-0.0090
12	0.122-0.061	.0005	48.350	60.00-90.00	0.0042-0.0060
10	0.100-0.050	.0005	59.010	75.00-110.00	0.0030-0.0041
8	0.080-0.040	.0003	73.840	90.00-140.00	0.0018-0.0026
7	0.065-0.0325	.00025	90.840	110.00-170.00	0.0012-0.0017
5	0.051-0.0255	.0002	115.750	140.00-220.00	0.00071-0.00107
4	0.043-0.0215	.0002	137.520	170.00-260.00	0.00052-0.00075
3	0.034-0.0170	.0002	173.280	220.00-325.00	0.00035-0.00047